Environmental Science and Pollution Research (2024) 31:18209–18225
https://doi.org/10.1007/s11356-023-26690-2

APPLIED SOLAR ENERGY

Experimental investigation of an indirect solar dryer with PCM-integrated solar collector as a thermal energy storage medium

Abdullah Bareen[1] · Soumya Dash[2] · Paragmoni Kalita[1] · Kshirod Kumar Dash[1,3]

Received: 12 October 2022 / Accepted: 23 March 2023 / Published online: 11 April 2023

Abstract

An indirect-type forced convection solar dryer implementing a phase-changing material (PCM) as the energy-storing medium was designed, fabricated, and investigated in this study. The effects of changing the mass flow rate on the valuable energy and thermal efficiencies were studied. The experimental results showed that the instantaneous and daily efficiencies of the indirect solar dryer (ISD) increased with the initial increase in mass flow rate, beyond which the change is not prominent both with and without using the PCM. The system consisted of a solar energy accumulator (solar air collector with a PCM cavity), a drying compartment, and a blower. The charging and discharging characteristics of the thermal energy storage unit were evaluated experimentally. It was found that after using PCM, drying air temperature was higher than ambient air temperature by 9–12 ℃ after sunset for 4 h. Using PCM accelerated the process by which *Cymbopogon citratus* was effectively dried between 42 and 59 °C of drying air. Energy and exergy analysis of the drying process was performed. The daily energy efficiency of the solar energy accumulator reached 35.8%, while the daily exergy efficiency reached 13.84%. The exergy efficiency of the drying chamber was in the range of 47–97%. A free energy source, a large reduction in drying time, a higher drying capacity, a decrease in mass losses, and improved product quality all contributed to the proposed solar dryer's high potential.

Keywords Renewable energy dryer · Energy storage · Exergy efficiency · *Cymbopogon citratus*

Nomenclature

A	Collection area, m^2
C_p	Specific heat, kJ kg K^{-1}
$\dot{E}_{id}$	Inlet exergy, W
$\dot{E}_{od}$	Outlet exergy, W
$\dot{E}_{los}$	Loss exergy, W
$\dot{E}$	Exergy rate, W
g	Gravitational acceleration, m s^{-2}
h	Enthalpy, kJ kg^{-1}
f	Convective heat transfer coefficient, W m^{-2} K^{-1}
I	Solar radiation, W m^{-2}
L_F	Latent heat, J kg^{-1}
m	Mass, kg
$\dot{m}$	Mass flow rate of air, kg s^{-1}
Q	Heat rate, W
T	Temperature, ℃
T^*	Apparent sun temperature,K
T_0	Outlet temperature of the solar collector,℃
T_m	Melting temperature,℃
t	Drying time, h
V	Velocity, m s^{-1}
w	Specific humidity,g g^{-1}
w_R	Uncertainty in the result,
w_η	Uncertainty in the efficiency of solar collector,
w_{η_d}	Uncertainty in the efficiency of drying chamber,
w_{η_E}	Uncertainty in exergy efficiency of the drying chamber,
η_0	Optical yield (dimensionless)

Responsible Editor: Philippe Garrigues

✉ Kshirod Kumar Dash
kshirod@tezu.ernet.in

[1] Department of Food Engineering and Technology, Tezpur University, Tezpur, Assam 784028, India

[2] Centre for Management Studies, North Eastern Regional Institute of Science and Technology, Nirjuli, Arunachal Pradesh 791109, India

[3] Department of Food Processing Technology, Ghani Khan Choudhury Institute of Engineering and Technology (GKCIET), Malda, West Bengal 732141, India

Greek symbols

$\alpha\tau$	Absorbance-transmittance product
η_E	Exergetic efficiency of drying chamber %
Δt	Difference in time
φ	Night-time useful heat
ψ	Exergy efficiency of solar collector (%)

Subscripts

o	Outlet flow
Amb	Ambient conditions
F	Fusion
ch	Charging process
dis	Discharging process
ini_ch	Initial charging process
ini_dis	Initial discharging process
fin_ch	Finish of charging process
fin_dis	Finish of discharging process
d	Drying chamber
r	Reference
i	Inlet, inflow

Introduction

Solar energy is a viable source for drying agricultural products due to the rising demand for clean energy. Compared to open sun drying (OSD), solar dryers can generate higher air temperatures and consequential lower relative humidity, conducive to improved drying rates and lower final moisture content of the drying crops (Mehta et al. 2022a). Besides from the above mentioned advantages of solar dryers, which indicate a significant advantage over conventional OSD, solar dryers also assist preserve energy by minimising the lag time between energy supply and demand.

Low-temperature drying is the most common way to preserve the quality of aromatic and medicinal plants. One such herb that can benefit from solar drying is lemongrass (*Cymbopogon citratus*), which is identified with its characteristic lemon flavor, prevalently produced for therapeutic uses, notably as tea, and its essential oil is highly desirable in the nutritional, pharmaceutical, cosmetics, and flavoring sectors (Nur Ain et al. 2013). Lemongrass leaves contain 78 to 82% citral, an aldehyde (Daniel 2006). Lemongrass is gaining prominence in the herbal sector, according to Mabai et al. (2018), because of its widespread usage as a cooking component. It has both floral and aromatic properties that provide an instant exotic appeal to food and beverages. But there are minimal studies on drying of lemongrass using an ISD combined with PCM that is energy efficient and preserves the product quality. Previous works have instead focused on the drying of lemongrass leaves in a solar dryer well as other dryers such as fluidized bed dryers, heat pump dryers, spray dryers, freeze dryers, and fixed bed dryers (Abd. Rahman et al. 2013; Cheenkachorn et al. 2022; Fadhel et al. 2010; Khaerunnisa et al. 2021; Martins et al. 2021; Mujaffar and John 2018; Thuong Nhan et al. 2020). Although most of these studies focus on various aspects of the drying process, such as quality and essential oil content (Alam et al. 2018; Alis et al. 2019; Boukhatem et al. 2022; Mabai et al. 2018), drying efficiency (Ebaid 2011), the effect of pretreatments (Balti et al. 2018; Kaur et al. 2021), and mathematical modeling of drying data (Karakaplan et al. 2019; Mujaffar and John 2018; Nguyen et al. 2019), they ignore the important factor of the best desired plants' drying temperature.

Various experimental and theoretical research works have been done in the last couple of decades, which have confirmed the excellent performance of solar dryers with thermal energy storage in the form of sensible, latent, or thermomechanical heat storage for drying many food products. Among them, latent heat storage materials are preferable because they have a high energy storage density per unit mass, require a small storage capacity, and suffer little losses while charging and discharging (Mehta et al. 2022b). Bhardwaj et al. (2017) investigated using an ISD with a phase change material (PCM), paraffin-wax as a source of latent heat storage for drying medicinal plants. Authors stated that PCM assisted in keeping drying air temperature 8–10 °C higher than ambient temperature for around 7 h by regulating the influence of inlet drying air temperature, sun intensity, surrounding air velocity, and relative humidity. By comparing solar drying with energy storage systems to heat pump drying and conventional OSD, they found that solar drying with energy storage system was 37.5% and 64.2% more efficient, respectively. Similarly, El Khadraoui et al., (2017) analyzed the potential for using paraffin wax to store solar energy during the day and release it at night. The solar energy accumulator was loaded with 60 kg of paraffin. During the drying non-sunny hours of operation, it was stated that the solar accumulator filled with paraffin wax assisted to keep the temperature 4–16 °C higher than the ambient temperature. There was an average energy efficiency of 33.9% and exergy efficiency of 8.5% for the solar accumulator. Since paraffin wax has been repeatedly recognized for its efficacy as a thermal heat storage source (Reyes et al. 2014; Shalaby & Bek 2014), it was chosen as the latent heat storage source for this investigation.

Indirect solar dryer (ISD) may make use of PCM in two different ways; the first, as proposed by Agarwal and Sarviya (2016) involves a heat storage unit served as a link between the heater and the drying area. The significant higher losses associated with such approach are its primary downside. Bhardwaj et al. (2021) proposed a second method in which the use of a solar air heater is equipped with a built-in PCM.

While the second scenario reduced the heat lost through the top surface, it still had significant losses throughout the system. ISDs using PCM storage designed using the minimum entropy generation method (Torres-reyes et al. 2001) are the focus of this investigation. Thermodynamic analysis for lowest entropy generation was used to compute all heat losses related to the ideal surface area of the storage unit, which is crucial for energy conversion processes that occur at limited rates, as these processes always create entropy. The solar dryer for this investigation were designed using our prior reports with thorough explanations of the flat plate solar collector's design and thermodynamic analysis as a reference point (Dash et al. 2022). This apparatus is intended to dry medicinal plants in the optimal drying air temperature. In contrast to prior approaches, this method eliminates all drawbacks.

There are multiple operating conditions and characteristics of a food product which can critically affect moisture removal rate and therefore overall performance of drying process. Therefore, the dryer performance results reported in literature deviate significantly. The performance analysis of solar dryers has got mainly two-fold objective: it serves as a measure of functionality and enables the calculation of the actual efficiency of the system under consideration. The results of the performance evaluation of the solar dryers can also be used for improvement in the design of the drying system.

The present paper is organized into six sections. The design of the experimental setup, along with the experimental procedure, is described in the "Description of the experimental procedure" section, followed by the methodologies for energy and exergy analyses in the "Methodology for the energy analysis" and "Methodology for the exergy analysis" sections, respectively. The "Results and discussion" section categorically presents the results and discussion through descriptions of the determination of optimum mass flow rate for the solar drying system, evaluation of drying indicator for lemongrass, evaluation of energy performance indicators for the solar drying system, and evaluation of exergy performance indicators for solar drying system. The concluding remarks after summarizing the findings of the present work are made in the "Conclusions" section.

Description of the experimental procedure

Raw material

Freshly harvested *Cymbopogon citratus* (lemongrass) samples were thoroughly washed and cleaned. *Cymbopogon citratus* was cut and spread in uniform thin layers of approximately 0.008 m thickness to ensure uniform drying. First, the spoiled grass was discarded to avoid product contamination from bacteria. Running tap water was used to clean the grass of any unwanted material. The sample was then placed in a stainless-steel mesh basket and drained for 1 min. The sample was weighed, squeezed, and reweighed. Samples with the same initial weight were weighed by an electronic balance in a laboratory (Make: K. Roy; Model: Dj-602A). The moisture content was calculated using the oven-drying method (Ranganna 1986). Three samples of *Cymbopogon citratus*, each of initial weight 5 g, were kept in the oven and dried at 105℃ for 24 h. The weight change was recorded every 60 min. The initial moisture level was calculated as 85% (wet basis). Paraffin wax, used as the PCM for solar drying, was procured from commercial suppliers from Guwahati, Assam, at a price of ₹66 per kg. It is a white or colorless soft solid derived from petroleum, coal, or oil shale that consists of a mixture of hydrocarbon molecules containing carbon atoms in the range of twenty to forty. It remains in the solid state at room temperature and begins to melt above approximately 37 °C (99 °F); its boiling point is > 370 °C (698 °F).

Experimental setup

A schematic layout and an image of the solar collector are shown in Fig. 1. The solar drying experiments were performed outdoors during March. To achieve a high solar irradiance, the collector is oriented toward the south direction at the local latitude of 26.8°. The collector setup was mounted on a suitably designed MS angle frame. Air temperature (ambient, collector outlet), radiation intensity, air velocity, and the drying chamber outlet temperature were measured. The major components of the solar collector were a cover plate, absorber plate, and base plate. For the absorber plate, an aluminum sheet of thickness 0.003 m painted black fitted into the box at a distance of 0.075 m from the cover plate was used. It was covered by a 0.005-m-thick transparent, Saint-Gobain make, toughened glass (emissivity and transmission coefficients are, respectively, 94% and 81% (Bouadila et al. 2014)), which acts as a cover plate. The PCM storage unit is located at the inner side of the absorber plate to reduce heat losses. Paraffin wax was used as a latent heat thermal storage in the PCM chamber. The heated air, after flowing through the tubes, was freely distributed in the drying chamber. A centrifugal blower having 0.025 m^3/s capacity was used to circulate the air through the solar dryer (Dash et al. 2022). The authors' prior work described the intricacies of the design technique for the solar collector, which was based on the mass flow number and least entropy generation number (Ns) (Dash et al. 2022).

Figure 2 shows a front view of the drying chamber (b) detailed schematic diagram of the drying chamber with the dimensions (c) image of the whole experimental setup

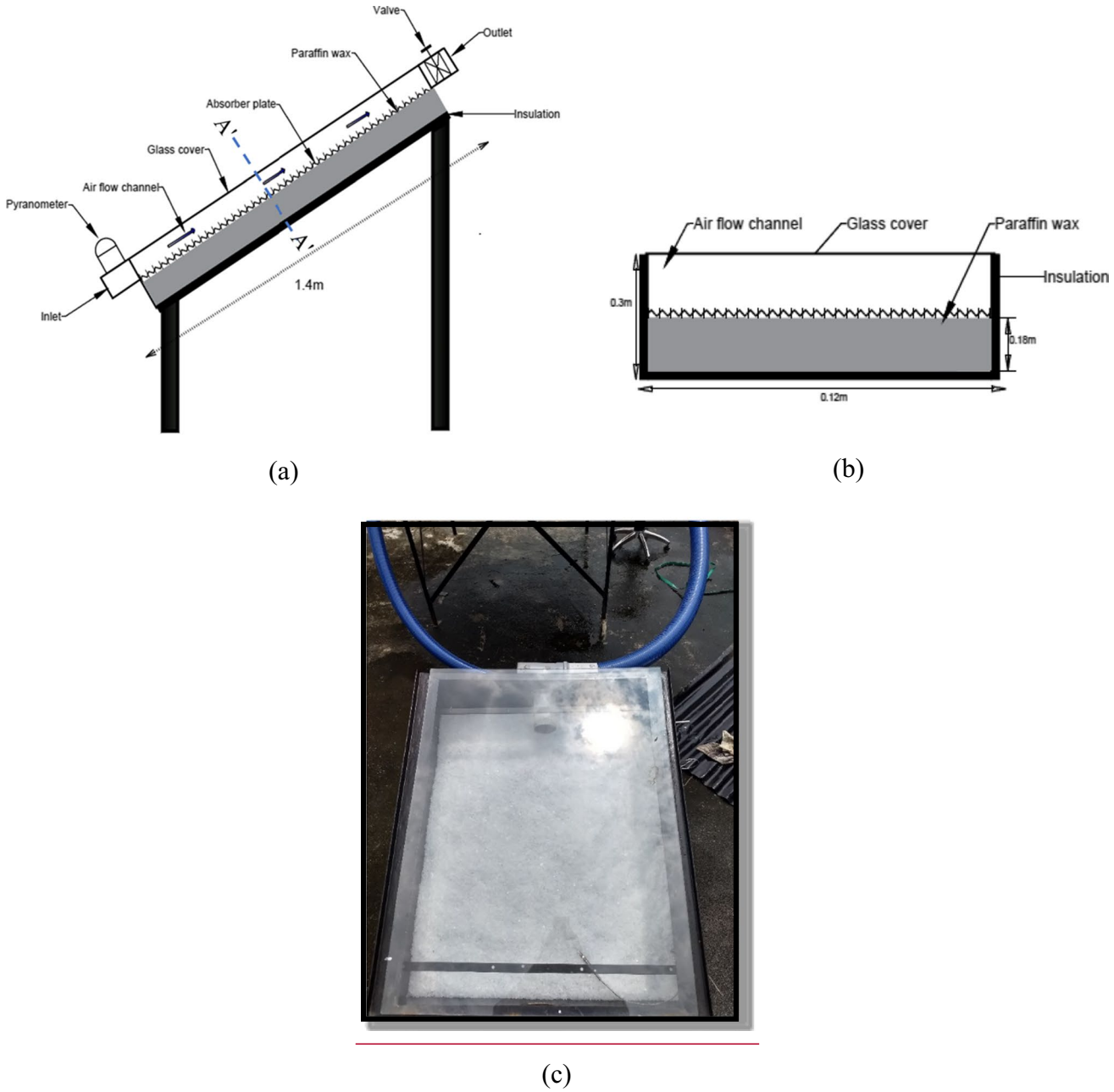

Fig. 1 A schematic diagram of the PCM-integrated solar collector (**a**) details of the dimensions of the experimental setup. **b** Cross section at A'-A'. **c** Photograph showing the top view of the solar plate collector filled with phase change material (PCM) in the thermal energy storage unit and attached PVC pipes for air flow to the drying chamber. The absorber plate was removed to detail the picture better

along with all the measuring instruments. The drying chamber was fabricated from galvanized iron with dimensions $0.9 \times 0.95 \times 0.95$ m^3 (length x width x height). On both sides and the bottom of the collector surface, the dying chamber was insulated with a layer of polyurethane (heat conductivity 0.028 W m^{-1} K^{-1}) with thicknesses of 0.15 m and 0.03 m, respectively. The drying chamber had three trays positioned at an equal vertical spacing of 0.27 m. The drying trays were made of aluminum to uphold the sample. The trays can be easily removed to load or unload the drying product from the door, representing one side of the drying chamber. A chimney was provided on the top of the drying chamber. The chimney increased the buoyancy force imposed on the air stream to provide a greater airflow velocity. Thus, a more rapid rate of moisture removal could be achieved (Ekechukwu and Norton 1999). PVC pipes of 0.0635 m with 0.002 m thickness were used to supply air from the collector to the drying chamber. The system was fully instrumented, and a special allowance

(a)

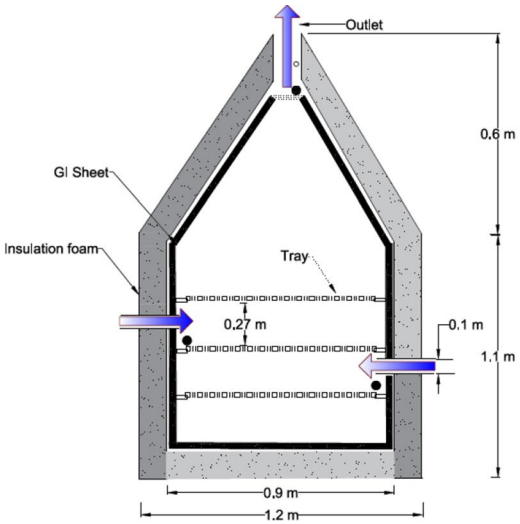

(b)

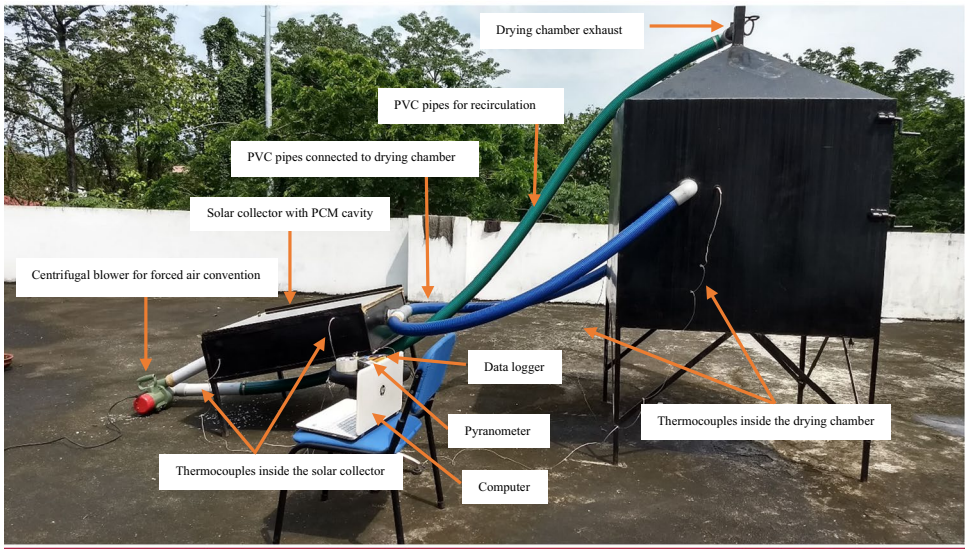

(c)

Fig. 2 Experimental setup. **a** Front view of the drying chamber with tray and dried lemongrass sample, **b** detailed schematic diagram of the drying chamber with the dimensions, **c** image of the whole experimental setup along with all the measuring instruments

was provided to measure the solar radiation properties and environmental parameters. The drying experiments were carried out in the developed solar dryer to determine the performance parameters at different mass flow rates of air. The lemongrass prior to drying and after drying in solar dryer and drying under open sun is presented in Fig. 3.

A: Raw lemon grass

B: Solar dried lemon grass

C: Open sun-dried lemon grass

Fig. 3 Lemongrass prior to drying and after drying in solar dryer and drying under open sun. **A** Raw lemon grass, **B** solar-dried lemon grass, **C** open sun-dried lemon grass

Measurements and experimental preparations

The temperature of the air at different locations of the drying system was measured with T-type thermocouples (WRNK-191, Packart Exim Pvt Ltd., India) during the experiments. The relative humidity (RH) of air at the inlet and outlet of the dryer and ambient air were obtained from the web bulb and dry bulb temperatures at the corresponding locations. The drying air characteristic instrument, as well as its accuracy, range, standard uncertainty, and uncertainty in measured variables, are detailed in Table 1. The experiments were divided into two cases to study the overall thermal performance of the ISD:

(a) Under no-load conditions, the solar dryer was tested without placing the lemongrass inside the dryer to determine the optimal mass flow rate for the maximum efficiency of the solar air heater, both with PCM and without PCM.
(b) With PCM under load, the solar dryer with paraffin wax was used to dry lemongrass to determine the energy and exergy during the process.

Methodology for the energy analysis

The energy analysis of the solar dryer is necessary to determine the extent of solar-energy utilization for heating the air and charging the PCM inside the solar collector. The first law of thermodynamics was applied to carry out the energy analysis based on the experimentally measured data.

The energy analysis is carried out in tandem with the mass-balance equation. The mass conservation of moisture can be written as Eq. (1) (Darvishi et al. 2014).

$$\sum \dot{m}_{ai} = \sum \dot{m}_{ao} = \dot{m}_a \tag{1}$$

$$\sum \left(\dot{m}_{wi} + \dot{m}_{mp}\right) = \sum \dot{m}_{wo} \tag{2}$$

In Eq. (2), $\dot{m}_{wi}$ and $\dot{m}_{wo}$ are the inlet and the outlet mass flow rates of moisture in the inlet and outlet air, respectively, $\dot{m}_{mp}$ is the mass flow rate of moisture of the product, w_i is the inflow-specific humidity, and w_o is the outflow-specific humidity.

The energy analysis for the dryer was carried out with the following assumptions:

i. The process was steady.
ii. All the thermo-physical properties of the air were constant in the operating range of the solar collector.
iii. The change in the potential energy of the air stream between the inlet and the outlet of the solar collector was negligible.
iv. Change in air velocities between the inlet and outlet was negligible.
v. The absorber plate was a black body.
vi. The cover did not absorb any amount of solar energy.

The thermal characteristic of the solar accumulator was obtained by writing the overall energy balance during both the charging and discharging process and is expressed by Eq. (3):

$$Q_A = Q_u + Q_{st} + Q_{los} \tag{3}$$

where Q_A,Q_u, Q_{st}, and Q_{los} are the absorbed, useful, stored (heat flux during charging and discharging phase), and lost energy, respectively.

The radiation absorbed by the absorber surface was estimated using Eq. (4).

$$Q_A = A(\alpha\tau)I \tag{4}$$

where $(\alpha\tau)$ is the effective product transmittance-absorptance. The useful heat gained by the air from the solar collector is calculated from Eq. (5) (Tiwari and Suneja 1997).

$$Q_u = \dot{m}_a Cp_a\left(T_o - T_i\right) \tag{5}$$

The heat stored by a latent heat storage system with a PCM medium during the charging and discharging phase is given as Eq. (6) and Eq. (7) (El Khadraoui et al. 2017):

$$Q_{ch} = \frac{1}{\Delta t_{ch}} m_{PCM}\left[\int_{in\_ch}^{F} Cp_s(T)dT + L_F + \int_{F}^{fin\_ch} Cp_l(T)dT\right] \tag{6}$$

Table 1 Uncertainties of measuring variables throughout the experimental works

Measuring device	Function	Uncertainty	Range
Type K thermocouples	Measuring air temperature	±0.5 °C	0–400 °C
Pyranometer	Solar insolation	±10 Wm^{-2}	400–1100 nm
Anemometer	Measuring air flow velocity	±0.25 ms^{-1}	0–50 ms^{-1}
Weighing balance	Moisture content	±0.025 kg water/kg dry matter on db	0–1000 g

$$Q_{dis} = \frac{1}{\Delta t_{dis}} m_{PCM} \left[\int_{in\_dis}^{F} Cp_l(T)dT + L_F + \int_{F}^{fin\_dis} Cp_s(T)dT \right] \quad (7)$$

The energy lost was obtained as shown in Eq. (8).

$$Q_{los} = Q_A - \left(Q_u + Q_{st}\right) \quad (8)$$

The thermal efficiency of the solar collector was calculated using Eq. (9) (Tiwari and Suneja 1997).

$$\eta = {}^{Q_u}/_{AI} \quad (9)$$

The night-time useful heat of the solar collector is defined as the ratio of desired energy output during the discharging process to the total energy input during the drying process, as shown in Eq. (10) (El Khadraoui et al. 2017).

$$\varphi = {}^{\int_{dis} Q_{dis}}\Big/_{\int_{ch} AI} \quad (10)$$

To calculate the uncertainties of the computed result in this study, uncertainty propagation analysis is used. Using the approach outlined by Kline (1953), the uncertainty of the computed findings are derived.

According to the method, if a result R is a given function of the independent variables x_1, x_2, x_3, $x_4 \ldots x_n$. Thus,

$$R = R(x_1, x_2 x_3 x_4 \ldots, x_n) \quad (11)$$

Then the uncertainty of R was given by Eq. (12):

$$\omega_R = \left[\left(\frac{\partial R}{\partial x}\omega_1\right)^2 + \left(\frac{\partial R}{\partial x_2}\omega_2\right)^2 + \left(\frac{\partial R}{\partial x_3}\omega_3\right)^2 + \ldots + \left(\frac{\partial R}{\partial x_n}\omega_n\right)^2 \right]^{1/2} \quad (12)$$

where R is a calculated result; $x_1, x_2 x_3 x_4 \ldots, x_n$ are measured values; $\omega_1, \omega_2, \omega_3, \ldots. \omega_n$ are the uncertainty of measured values $x_1, x_2 x_3 x_4 \ldots, x_n$, respectively; ω_R is the absolute uncertainty of result R; and ω_R/R is the percentage uncertainty of result R. The highest percentage uncertainty of the air heat gain, solar radiation, and collector thermal efficiency in this experiment is 1.12%, 6%, and 6.78%, respectively, according to the uncertainty equation. Table 1 shows the uncertainty of measuring tools employed throughout the drying test.

Methodology for the exergy analysis

The exergy of a solar dryer is defined as the maximum useful work possible during the drying process that brings the dryer into equilibrium with the heat reservoir. The exergy analysis uses the conservation of mass and the energy principles together with the second law of thermodynamics in the context of the drying system. Solar radiation, radiation intensity, and collector temperature affect the exergy efficiency of the solar dryer. The exergy losses associated with the drying chamber are the exergy loss with the air leaving the dryer, the exergy loss from the walls of the dryer due to heat rejection, and the exergy loss in the product (Dincer et al. 2007). The developed dryer is not continuous; therefore, the exergy loss in the product was neglected. The following assumptions were made during the exergy analysis.

- The flow was assumed to be steady.
- The effect of kinetic and potential energies was neglected.
- The effect of moisture content on the heat capacity of air leaving the dryer was neglected.

Therefore, the steady-state exergy flow rate can be expressed as Eq. (11).

$$E = \dot{m}_a \left[Cp\left(T - T_r\right) - T_r \left\{ Cpln\left(\frac{T}{T_r}\right) - R\ln\left(\frac{P}{P_r}\right) \right\} \right] \quad (11)$$

where T_r is the reservoir temperature and P_r is the reservoir pressure. The change in the pressure between the inlet and exit of the dryer is negligible. Accordingly, Eq. (11) can be written as:

$$E = \dot{m}_a Cp_a \left[\left(T - T_r\right) - T_r ln\left(\frac{T}{T_r}\right) \right] \quad (12)$$

Therefore, the drying chamber's exergy inflow and outflow rate were determined using Eq. (13) and Eq. (14), respectively.

$$E_{id} = \dot{m}_a Cp_a \left[T_{id} - T_r - T_r ln\left(\frac{T_{id}}{T_r}\right) \right] \quad (13)$$

$$E_{od} = \dot{m}_a Cp_a \left[T_{od} - T_r - T_r ln\left(\frac{T_{od}}{T_r}\right) \right] \quad (14)$$

The exergy loss in the dryer was obtained by

$$E_{ls} = E_{id} - E_{od} \quad (15)$$

The exergy efficiency of the drying chamber is defined as the ratio of exergy outflow to the exergy inflow of the drying chamber (Rabha et al. 2017). It was calculated based on Eq. (16).

$$\eta_E = \frac{E_{od}}{E_{id}} \quad (16)$$

The absorbed solar radiation exergy rate, assuming the sun as an infinite thermal source, was calculated using Eq. (17) (Torres-reyes et al. 2001; Öztürk 2004):

$$E_{in}(absorbed) = \eta_0 IA\left(1 - \frac{T_a}{T^*}\right) \quad (17)$$

The stored exergy rate is both sensible and latent change within the PCM for the charging state, so it becomes in the discharged process, which can be given by Eq. (18) (MacPhee and Dincer 2009):

$$E_{dis} = \frac{1}{\Delta t_{dis}}\left[m_{PCM}Cp_l\left\{T_m - T_{fin\_dis} - T_a\ln\left(\frac{T_m}{T_{fin\_dis}}\right)\right\} + m_{PCM}L\left(1 - \frac{T_a}{T_m}\right) + m_{PCM}Cp_s\left\{T_{ini\_dis} - T_m - T_a\ln\left(\frac{T_{ini\_dis}}{T_m}\right)\right\}\right] \quad (18)$$

The exergy efficiency of a solar collector is the ratio of the net exergy recovered during the discharging processes by the total required exergy input to the solar collector, which was estimated using Eq. (19) (El Khadraoui et al. 2017):

$$\psi = \frac{E_{dis}}{E_{in}(absorbed)} \quad (19)$$

Results and discussion

Energy analysis was carried out to estimate the amounts of energy gained from solar air collectors and the ratios of energy utilization. To investigate the thermal performance of the solar dryer, the device was first tested under no-load conditions. The optimal mass flow rate of air through the solar dryer was determined for maximum energy and exergy efficiencies. After that, the air mass flow rate thus defined for the solar dryer with a thermal storage system was utilized to dry lemongrass. The drying experiments were conducted from 8:00 h to 17:00 h during the day hours. At night, the drying experiments continued through 17:00 h and finished at 21:00 h.

Determination of optimum mass flow rate for the solar drying system

To optimize the accumulation of solar radiation and ensure air supply into the drying chamber, the collector was directed at a local latitude of 26.8° toward the south direction. The variations in ambient conditions recorded for no load experiments in no PCM (NPCM) and with PCM modes are shown in Fig. 4. Ambient air temperature recorded every hour from 8:00 to 21:00 h is shown in Fig. 4a. Furthermore, solar radiation for 6 consecutive days recorded using the data logger every 6 min using the pyranometer during the experiments is shown in Fig. 4b. During the investigation, both scenarios are compared under similar ambient circumstances. The ambient air temperature was the same as the inlet temperature of the solar collector; the recorded values were in the range of 24.9 to 32.2℃, with an average of 28.3, 28.8, and 28.5 ℃, respectively, during the 3 consecutive days. The solar radiation intensity recorded during the first 3 days of the experiments for NPCM mode varied in the range 257.85 to 933.84 W/m^{2}K, with an average of 649.18, 755.09, and 733.5 W/m^{2}K for 3 consecutive days, respectively (Fig. 4b). The maximum solar radiation intensity was recorded between 11:00 and 13:00 h. The measured inlet temperatures of the solar collector follow the solar intensity as they increase gradually to reach their peak and then start to decrease gradually. The solar radiation during the PCM mode experiments varied from 292 to 888 W/m^2, averaging 716, 668, and 721 W/m^{2}K, respectively, during the 3 consecutive days. The maximum solar radiation intensity was recorded between 12:00 and 13:00 h. The measured ambient temperature of the ISD with the PCM follows the solar intensity discussed in Fig. 4b. The outlet temperature of the solar collector was also recorded for each day. Governed by these conditions, the ISD in NPCM and PCM modes was tested for 6 consecutive days (3 days for each mode) under varying air mass flow rates from 0.02 to 0.08 kg/s for each day to determine the optimum mass flow rate for maximum thermal performance.

Table 2 illustrates the effect of changing air mass flow rates on the useful energy and the thermal efficiency of the ISD without PCM. The useful energy of the solar dryer was estimated for each hour during the experiment. The total useful energy was the sum of all the useful energy gained during each hour at a particular mass flow rate throughout the day. The solar dryer's total useful energy (Eq. (5)) ranged from 1408.58 to 5986.52 W within mass flow rates of 0.01 and 0.14 kg/s, respectively (Table 2). It is seen from Table 2 that the maximum value of the total useful energy obtained by the ISD calculated was 5986.52 W, respectively. The hot air temperature inside the drying chamber was slightly lower than that of the collector outlet temperature under NPCM mode. Some heat energy is used to carry hot air from the collector outlet to the drying chamber. It was observed that at all mass flow rates, the thermal efficiency, and useful energy increased gradually with increasing solar intensity and ambient air temperature and achieved the maximum values of 11:00–13:00 h, which gradually decreased beyond that and finally became zero at sunset. When the mass flow rate increased, the total useful energy increased sharply until the mass flow rate reached 0.08 kg/s. It was also observed that beyond this air mass flow rate, the increment of total useful energy was not prominent. This indicated that the performance of the installed solar dryer in the NPCM mode was efficient when operated at a mass flow rate of 0.08 kg/s, which is in good agreement

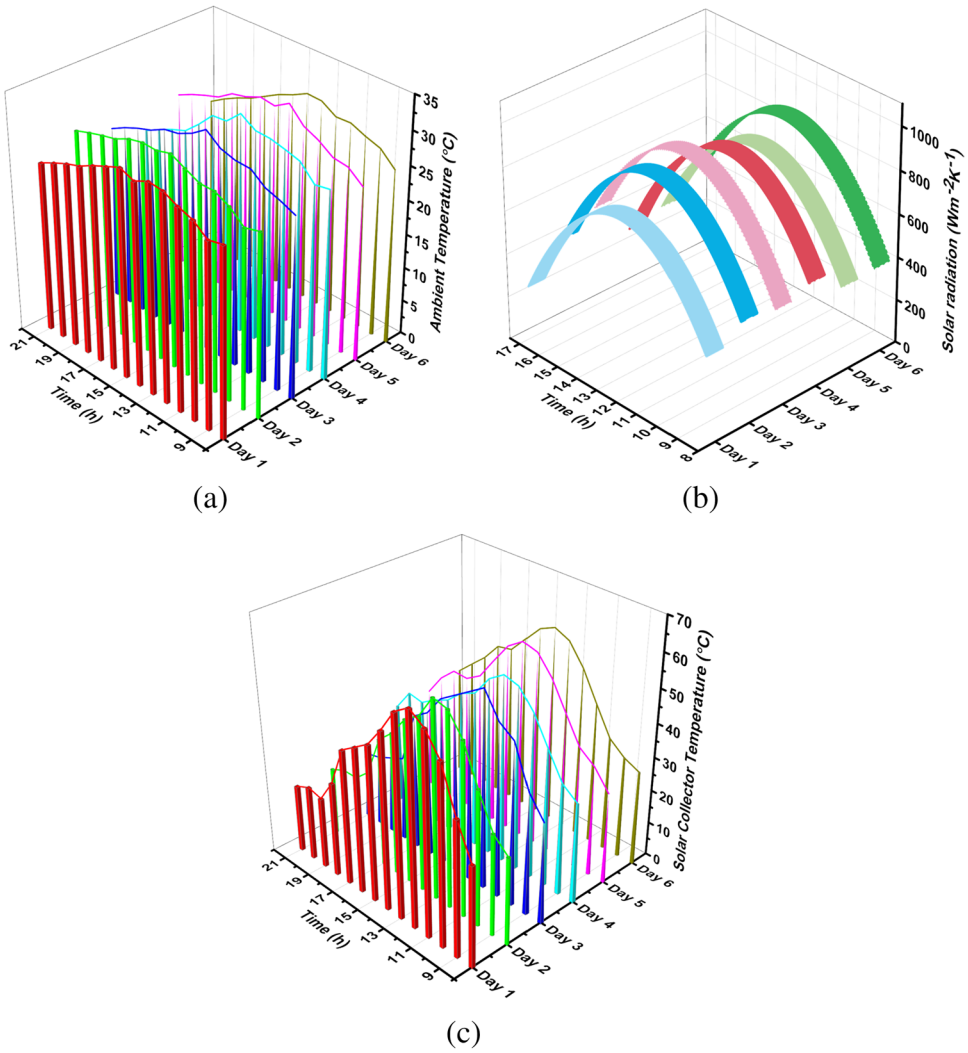

Fig. 4 The drying experiment for NPCM (days 1–3) and PCM (days 4–6) modes of the solar dryer. **a** Ambient air temperature, **b** solar radiation, **c** solar collector outlet temperature

Table 2 The effect of changing the mass flow rates of air on the useful energy and the thermal efficiency of the indirect solar dryer NPCM and PCM modes

Mass flow rate (kg/s)	Useful energy (Q_u) (W)		Thermal efficiency (η) (%)	
	NPCM	PCM	NPCM	PCM
0.02	1408.5	1641.6	13.1	20.26
0.05	4481.4	6297.3	75.4	76.53
0.08	5986.5	6603	75.4	81.6

with the results obtained from the literature (Esakkimuthu et al. 2013). In a related investigation on the thermal performance of a double pass-finned plate solar heater with different mass flow rates of air, the peak values of the thermohydraulic efficiencies of the dual pass-finned and V-corrugated plate solar air heaters were obtained when the mass flow rates of the flowing air were 0.0125 and 0.0225 kg/s, respectively (El-Sebaii et al. 2011). Moreover, the results from a twin study on the thermal performance comparisons between a flat and V-corrugated plate solar air heater revealed that the peak values of the thermohydraulic efficiencies of the flat and V-corrugated plate solar air heaters were obtained when the mass flow rate of the flowing air was 0.02 kg/s. Testing the dryer's functionality before putting it to use with the items to be dried is a crucial step after the ISD's appropriate design. The no performance index load (NLPI) parameter is commonly used to assess performance. (Mehta et al. 2018). The mathematical model for NLPI for the designed drier can be given as (Mehta et al. 2018): $\dot{m}_a Cp_a/Af$. The NLPI of the system with the average ambient air temperature 28.3, 28.8 and 28.5 ℃ for day 1, 2 and 3 was calculated as 1.84, 1.88 and 1.85, respectively. The authors Singh and Kumar (2012) reposted NLPI for ISD operated in forced convection mode with the mass flow rate of 0.026 kg/s, and ambient air temperature of 27.87 °C was 1.48.

To investigate the influences of the PCM on the performance of the indirect solar collector, the dryer was also tested using 10 kg of the PCM with the same airflow rates for 3 consecutive days from 8:00 to 21:00 h. Table 2 shows

the effect of changing the mass flow rates of air on the useful energy of the ISD with PCM. The ISD was tested with PCM by varying the airflow rates of air from 0.01 to 0.14 kg/s. The total useful energy of the ISD was obtained from Eq. (5). The total useful energy varied from 1641.63 to 6603 W. From Table 2, it can be seen that the total useful energy increased with increasing the mass flow rate but only up to mass flow rate of 0.055 kg/s. Beyond this mass flow rate, the rates of change in the total useful energy were insignificant. This might be since the mass flow rate for a specific area of the thermal collector is constant, and any mass flow rate higher than that is pointless since it would not be able to stay in the collector long enough for heat transfer to occur. This revealed that the high thermal performance of the solar dryer with PCM could be achieved if operated at a mass flow rate of 0.055 kg/s.

The useful energy values followed the exact shape of the solar radiation curve until sunset. Still, they then again increased to reach a maximum value as time advanced until 4 h. The later increase in the useful energy was due to a large amount of recovered thermal heat from the PCM during the discharging process that started when the sun began to fade. However, filling the collector with PCM at the bottom noticed almost constant temperature. This was because PCM absorbed the excess heat of the day and supplied it to the drying chamber when there was a fall in the drying temperatures. Hence, by changing its phase, it ensured constant temperature for longer durations. The temperature of the PCM remains approximately constant during the melting and solidification period. It was observed that the melting process started at 14:00 h when the PCM temperature reached 63℃. During the melting process around this temperature, part of the absorbed solar energy was stored within the PCM. This stored energy was recovered after sunset (discharging process). So, the outlet air temperature remained higher than the ambient temperature for 4 h at night. During this time, the PCM was considered the only heat source in the system because it rejected large heat during its solidification process. The PCM solidification process started at 17:00 h when the sun began to fade, and the PCM mean temperature attained a higher value than the ambient. The results indicated that the charging (8:00–14:00 h) and discharging (15:00–21:00 h) time was 6 h.

The PCM provided a uniform drying temperature to the chamber. This moderated drying temperature was suitable for drying spices, especially those containing volatile oil. The initial results showed that the optimum mass flow rate of air required decreased to 0.055 kg/s when the solar dryer was tested with paraffin wax as a heat storage medium. This could be because the sum of useful energy produced in a day was more significant than when the solar dryer was tested without any thermal storage medium. The increase in the sum of useful energy can be correlated to the ability of the paraffin wax to store heat during the peak-sunshine hours, which was then used to heat the air inside the solar collector during off-sunshine hours. The amount of useful energy produced during the experiments with the ISD at a similar mass flow rate was higher with paraffin wax inside the collector. Therefore, a mass flow rate of 0.055 kg/s was chosen for the ISD's solar drying of *Cymbopogon citratus*.

The total thermal efficiency was the average of the thermal efficiency of the solar dryer all through the day, calculated over each hour at a specific mass flow rate. The total thermal efficiency (Eq. (9)) during the test period for NPCM varied from 13.19 to 75.41% at mass flow rates of 0.01 kg/s and 0.08 kg/s, respectively (Table 2). Similarly, the sum of the total thermal efficiency of the solar dryer for 3 consecutive days of experimentation in PCM mode varied from 20.26 to 81.6% (Table 2). The effect of using paraffin wax as the thermal storage medium is shown in Fig. 4c. It can be observed that the system with PCM stayed in operation until 21:00 h (4 h after sunset). Moreover, after sunset hours, the efficiency values of the ISD were higher than those of the solar dryer in NPCM mode. The thermal efficiency is conferred based on the energy gathered by the collector. Therefore, the efficiency increases with the increase in the rate of solar radiation. The increase in efficiency was the highest at 13:00 h when the solar radiation rate was the maximum. The average collector efficiency of the dryer in PCM mode at a mass flow rate of 0.055 kg/s was 13% higher than in NPCM mode. This is due to the increase in the value of the heat transfer coefficient at a higher mass flow rate associated with the reduction in the heat losses, in addition to the decrease of the average temperature of the collector. The increase in the useful energy and thermal efficiency of the solar collector due to the use of PCM has been investigated experimentally by many researchers. An experimental study of a novel solar dryer using paraffin wax as a PCM revealed that the drying air temperature was higher than the ambient air temperature by 2.5–7.5 ℃ after sunset for 5 h (Shalaby and Bek 2014). The system's main components were two identical solar air heaters, a drying chamber, PCM storage units, and a blower. The solar dryer was tested under no load with and without PCM. Two cylindrical plastic containers with a height of 0.3 m and an inner radius of 0.15 m were filled with PCM (paraffin wax) and were fixed to the bottom of the drying chamber. It was found that the drying air temperature in the solar dryer with PCM, after 14:00 h, was 3.5–6.5 ℃ more than that without a PCM. In another study, the thermal performance of the finned plate solar air heater (FPSAH) was investigated experimentally by using paraffin wax as a PCM under the weather conditions of Tanta town. The experimental results showed that the collector efficiencies of the FPSAH with and without the PCM increased when the mass flow rate increased. It was concluded that using phase

change material by the finned plate solar air heater improved the collector efficiency by 10.8–13.6%.

Similarly, experimental investigations on the flat and V-corrugated plate solar air heaters with built-in paraffin wax as thermal energy storage material were conducted under prevailing weather conditions of Tanta, Egypt. It was found that when using the PCM, the outlet temperature of the V-corrugated plate solar air heater was higher than ambient temperature by 1.5–7.2 ℃ 3.5 h after sunset compared with 1–5.5 ℃ 2.5 h after sunset for flat plate solar air heater when the mass flow rate was 0.062 kg/s. It was also concluded that the sum efficiency of the V-corrugated solar heater using PCM was 12% higher than the corresponding ones without using the PCM, and it was also 15% and 21.3% higher, respectively, than the corresponding values for the flat plate collector with and without PCM at a mass flow rate of 0.062 kg/s, respectively.

Evaluation of drying indicator for lemongrass

The drying experiments of *Cymbopogon citratus* were performed for 2 consecutive days, starting from 8:00 to 21:00 h. The variations in the solar radiation, ambient temperature, and solar collector outlet temperature for 2 successive days during the time of experimentation are shown in Fig. 5a. During the test period of drying *Cymbopogon citratus* in the indirect solar collector, the solar radiation intensity varied from 267.76 to 953.08 W/m^2 with an average of 660 W/m^2 on day 1 and 689 W/m^{2}k for day 2. The maximum solar radiation intensity for both days was recorded between 12:30 and 14:00 h. The ambient temperature was in the range of 22.3 to 39.0℃ with an average of 33 ℃ and 31 ℃ for day 1 and day 2, respectively. The solar collector outlet temperature was 21.2 to 54.2 ℃ with an average of 43℃ for both days of drying *Cymbopogon citratus*. The maximum temperature difference was 12.9 ℃ and 12.6 ℃ during the first and second drying days, respectively. Due to the integration of thermal energy storage, the temperature inside the dryer was maintained at least 9–12℃ more than the ambient temperature for 4 h after sunset on each day. The inlet temperature of the air entering the thermal storage mainly depends on the solar radiation intensity. This is because the drying air inside the thermal storage was drawn from ambient air and heated by solar radiation. When the solar radiation falls, the ambient temperature decreases; hence, the inlet temperature of the solar collector is also lower. The maximum temperature of the thermal energy storage was measured as 58.9℃ at 12:30 h and 57.6℃ at 14:00 h during the drying of *Cymbopogon citratus* on the first and second day, respectively. During the morning hours, the temperature of the air entering the solar collector was higher than the temperature of the wax; hence, the charging occurred. The recorded maximum temperatures of PCM during the experiments were achieved around 13:00 h for both days. This implied charging process of paraffin wax took place from morning 8:00 to 14:00 h. The sudden temperature drop can establish the discharging process during the initial period of discharging due to the release of sensible heat. The rapid release of heat during the starting of discharging process is due to the temperature difference between solar collector inlet air and PCM, which is the necessary driving power for heat transfer. The discharging of paraffin wax increased the solar collector outlet temperature of the air during the off-sunshine period and maintained higher than the ambient temperature. The paraffin wax temperature was high at the start of the discharge process, and the PCM was in a liquid state. At this state, sensible heat was discarded from the PCM as the temperature dropped from 58.9 to 48.3 ℃ and from 57.6 to 47.5 ℃ on day 1 and day 2 of the experimentation, respectively. During this time, there was convection-driven heat transfer in the molten PCM. As the PCM reached the solidification temperature, the solidification started and proceeded into a phase change-controlled period. The PCM layer, which was in contact with the solar collector inlet air, began to freeze and discharge its latent heat.

The primary resistance to heat transfer during this process was due to the transfer of heat from the inner paraffin wax to the outside. Hence, we found that PCM released its sensible heat very rapidly, and then a longer time is needed to transfer latent heat during the phase change. The latent heat stored in the PCM was a significant portion of its dissipated heat (Torres-reyes et al. 2001). The temperature of the PCM dropped from 58.9 to 45.3 ℃ in approximately 400 min. During this duration, latent heat was released from the PCM to the air inside the solar collector. For safe storage of *Cymbopogon citratus*, the moisture content was reduced to 8.0% (wb) from its initial moisture content of 88.14% (wb) in 26 h in the drying air temperature range of 42–59 ℃. Similar results were obtained using the forced convection ISD integrated with phase change material; it took 30 h to dry *Cymbopogon citratus*, whereas traditional sun drying needed 4–5 days (Janjai et al. 2002).

The variation of experimental and predicted moisture ratio of *Cymbopogon citratus* with drying time is presented in Fig. 5b. Using phase change material, the drying air temperature inside the drying chamber supplied from the solar collector was sufficiently high compared to the atmospheric temperature, and corresponding humidity was lower than the ambient air. By adopting this technique, phase change material permitted hot air at a higher temperature to *Cymbopogon citratus* placed on the trays and maintained a temperature difference with the ambient atmospheric air. Phase change material absorbed excess heat above 40 °C and released the same when there was a fall in drying air temperature. The rate of moisture loss from *Cymbopogon citratus* decreased with the increase in drying time until the sample approached

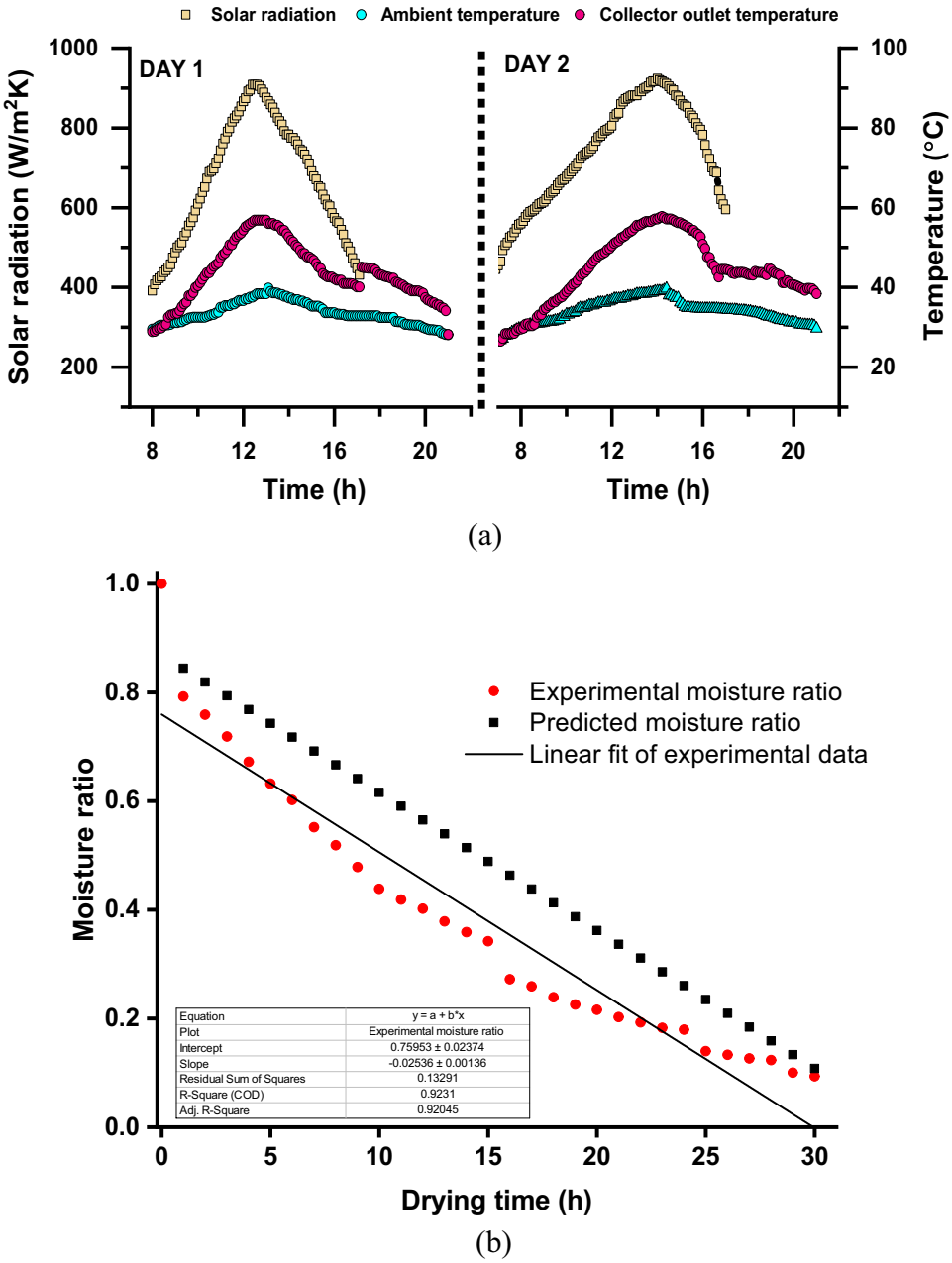

Fig. 5 Drying *Cymbopogon citratus* in the solar dryer (**a**) ambient conditions and the collector outlet temperature (**b**) variation of experimental and predicted moisture ratio of *Cymbopogon citratus* with drying time

the equilibrium moisture content (EMC). The drying mainly happened in the falling rate period, indicating a diffusion-controlled drying mechanism. Similar results were reported by Ibrahim et al. (2009), indicating that the drying air temperature increased the drying process and decreased the EMC of lemongrass. Initially, the weight loss of *Cymbopogon citratus* was faster because of the free moisture content on the outer surface and then gradually became slower due to the movement of moisture from internal layers to the outer surface and finally gets saturated (Ibrahim et al. 2009). A similar trend was observed during an experimental investigation of an ISD integrated with phase change material for drying *Valeriana Jatamansi* (Chauhan et al. 2017).

Evaluation of energy performance indicators for the solar drying system

The variation of absorbed, useful, and stored energy as functions of drying time during the solar dryer experiments for drying *Cymbopogon citratus* is illustrated in Fig. 6. Most of the absorbed solar energy was stored inside the PCM cavity. The useful heat values calculated using Eq. (5) during the drying of *Cymbopogon citratus* in the ISD with PCM during the 2 days (for day 1 and day 2) varied from 0.04 to 0.83 kW and 0.003 to 0.99 kW, respectively. It could be noted that during the initial period of charging, the heat stored increased with the solar radiation and reached its

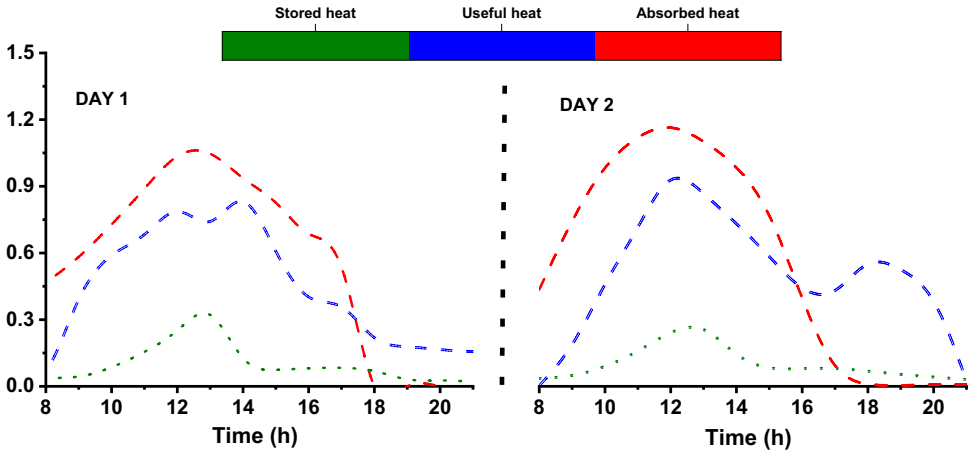

Fig. 6 The variation of absorbed useful and stored energy as functions of drying time: **a** day 1, **b** day 2

peak value of 0.28 kW at 12:30 h on day 1. At this time, the absorbed heat (Eq. (4)) was 1.04 kW on the same day. During the discharging process of the PCM, the useful heat (Eq. (5)) was uniform for a more extended period with an average value of 179 W/m^2.

Similarly, during the second drying day, the heat stored (Eq. (5)) reached its peak value of 0.32 kW at 13:00 h. During the same time (13:00 h), the absorbed heat reached 1.18 kW. During the second day of the drying process, the night-time useful heat had an average value equal to 395.56 W/m^2. This was the primary advantage of solar collectors integrated with PCM units, where a uniform discharging process was possible for an extended period, which could help dry crops. A comparative study has been done between some previous research works and the current study on the results obtained during the energy analysis of solar dryers developed for drying different crops. In the present study, from the energy analysis, it was seen that the solar dryer with 10 kg of paraffin wax helped keep a part of the absorbed energy on day 1 of the experiments after sunset, contributing to 0.71 kW energy being generated for drying and maintain the drying chamber temperature at 9–12℃ higher than the ambient temperature for 4 h after the sunset. An ISD that utilized a phase change material was developed by Reyes et al. (2014) for the dehydration of mushrooms. The main components of the solar dryer were a solar panel, a solar energy accumulator, a centrifugal fan, an electrical heater, and a drying chamber. The solar energy accumulator contained 14 kg of paraffin wax, which was used as a heat storage medium distributed in 100 copper pipes with external aluminum fins that favored the heat transfer to the drying air. Their results showed that using the solar energy accumulator reduced electrical energy consumption in the range of 40 to 70%. The maximum energy fraction supplied by the accumulator to the drying process was 0.20. Incorporating PCM contributed significantly to improving the global thermal efficiency of the system, and mushrooms were successfully dehydrated, which helped maintain a higher hardness than fresh mushrooms (Reyes et al. 2014). In a similar experimental study on the performance of an ISD equipped with a latent storage system to maintain the continuity of drying of herbs for their color and flavor vulnerability (Jain and Tewari 2015), it was found that the drying air temperature in the chamber was 6 ℃ higher than the ambient temperature after the sunshine hours until midnight during June at Jodhpur (India). The solar dryer consisted of four major parts: a flat plate collector, a packed bed for thermal storage, a drying chamber, and a natural draft system. The phase change material (48 kg of paraffin wax) was stored in 48 cylindrical tubes placed over the drying plenum to build the thermal buoyance for the natural convection of moist air during off-sunshine hours. The tubes were 0.75 m in length and had a diameter of 0.05 m (Jain and Tewari 2015).

The night-time useful energy (Eq. (10)) was calculated as the sum of the useful energy obtained during the operation of the ISD after sunset hours. The night-time useful energy is the ratio of desired energy output during the discharging process to the total energy input during the charging process. Day 1 of the studies using NPCM mode provided the ambient circumstances for acquiring the energy indicators under no load conditions. For the solar dryer with load, the values of the absorbed heat, night-time useful heat, and exergy efficiency calculated during the day 1 drying of *Cymbopogon citratus* were considered. For solar drying with load, during the day 1 drying of *Cymbopogon citratus*, the daily absorbed heat was 8.16 kW. The night useful heat was 0.71 kW (Table 3). A similar study aimed at investigating the feasibility of using a solar air heater to store solar energy during the daytime and to release it at night has been carried out by researchers at the Research and Technology Center for Energy, Tunisia (El Khadraoui et al. 2017). The major components were solar air, a panel for direct heating of the drying agent, a solar energy accumulator (solar air collector with PCM cavity), and a drying chamber. They reported that

Table 3 Daily absorbed heat, daily useful heat, and daily energy and exergy efficiency for solar collector

Indirect solar dryer mode	Absorbed heat (kW)	Night-time useful heat (kW)	Daily exergy efficiency (%)
Under no load	8.10	-	12.1
With load	8.16	0.71	28.38

the daily energy efficiency and the daily exergy efficiency of the solar energy accumulator reached 33.9% and 8.5%, respectively.

Evaluation of exergy performance indicators for the solar drying system

The exergy analysis of the thin layer drying process of *Cymbopogon citratus* via the forced solar dryer was performed using data obtained from the drying experiments. The variation of exergy inflow, exergy outflow, exergy loss, and exergy efficiency, with time for day 1 and day 2 of the conducted drying experiments, is shown in Fig. 7. The exergy inflow and outflow (Eqs. (13)–(14)) of the dryer varied from 8.78 to 26.87 W and 2.06 to 17.3 W, respectively. The exergy loss E_{ls} (Eq. (15)) varied between 1.24 and 11.28 W during the experiments on drying lemongrass. The dryer's exergy efficiency (Eq. (16)) ranged from 21.85 to 97.26%. These values show that the exergetic efficiency of the drying chamber decreased while the energy taken from the solar collector was productively utilized. It was observed that the exergy efficiency was low at the start of the drying process of the next day after the interruption during the night period. The exergetic efficiency of the drying chamber increased with the decrease in the temperature difference between the inlet and outlet of the dryer chamber. There was a swift increase in exergy efficiency in the first hour and then almost remained constant for the next 3 h. It again started increasing in the last 3 h. In a study on a forced convection solar tunnel dryer integrated with a shell and tube-based latent heat storage module for drying Ghost chili pepper and sliced ginger, a similar pattern of the exergy efficiency curve for the solar drying process of Ghost chili pepper in the fabricated solar dryer was reported (Rabha et al. 2017).

In the drying experiments at a mass flow rate of 0.055 kg/s, the exergy loss in the drying chamber increased during the first 7 h and decreased gradually. Such time variation of the exergy loss appeared as a consequence of the changes in solar radiation. Hence, the air had more exergy at the chamber outlet than the inlet air leading to high exergy efficiency in the latter part of the day. From a thermodynamic point of view, the exergy outflow from the drying chamber was seen as a section that negatively affected the system's exergy efficiency. Fudholi et al. (2014) reported

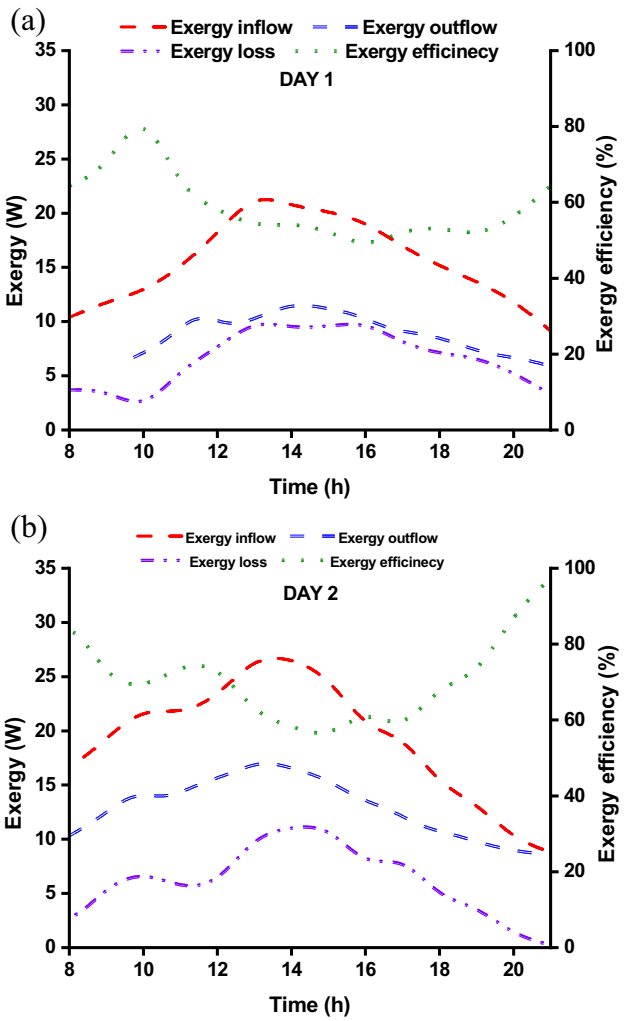

Fig. 7 The variation of exergy inflow, exergy outflow, exergy loss, and exergy efficiency as a function of drying time: **a** day 1, **b** day 2

a similar exergy efficiency curve pattern for red seaweed's solar drying process. The results showed the exergy efficiency of solar drying ranged from 31 to 93%, with an average of 72.08% (Fudholi et al. 2014). Similar results were reported for the energy and exergy analyses of the drying process of olive mill wastewater (OMW) using an indirect-type natural convection solar dryer. Olive mill wastewater dried sufficiently at temperatures between 34 and 52 ℃. During the 2 days of the experimental process, the exergetic efficiencies of the drying chamber varied from 34.4 to 100% (Celma and Cuadros 2009). An experimental study was conducted to carry out the energy and exergy analyses of the thin layer drying process of mulberry via a forced solar dryer where the drying experiments at five different drying mass flow rates varied between 0.014 and 0.036 kg/s and that the exergy of thin layer drying process of mulberry via the forced solar dryer varied from 21.3 to 93.3% (Akbulut and Durmuş, 2010). A solar drying system was designed

by Fudholi et al. (2014) for the drying of red seaweed. The energy and exergy analyses were performed, and the results showed that the ISD's efficiency varied from 47 to 97% (Fudholi et al. 2014).

Table 3 shows the daily exergy efficiency of the ISD when operated without load and with the load. A solar collector's average daily exergy efficiency is the ratio of the net exergy recovered during the discharging processes to the total required exergy input to the solar collector. Under no load condition, the experimental values of absorbed heat and daily exergy efficiency for the ISD without PCM were calculated using Eq. (4) and Eq. (19), respectively, at the solar radiation intensity range of 343.25 to 931.52 W/m^2. The average value of daily exergy efficiency of the ISD under NPCM mode (for ambient conditions as illustrated in Fig. 4) was around 12.1%, and the average value of daily exergy (day 1) efficiency when the solar dryer was used for drying *Cymbopogon citratus* (for ambient conditions illustrated in Fig. 5a) was calculated as 28.38%.

Conclusions

The performance of a new ISD performance was investigated in two different cases. In the first case, the solar dryer was tested using a phase-changing material (PCM), and the second was when the device was tested without the PCM. The experimental results when using the PCM indicated a higher temperature difference of drying air since it successfully maintained the drying temperature at an approximately constant value for eight consecutive hours per day. In addition, it provided a moderate drying air temperature, so it was suitable for drying spices, especially those containing volatile oil. Operating the ISD with mass flow rates of 0.055 kg/s and 0.08 kg/s gave the peak value of drying air temperature when the dryer served with and without PCM, respectively. *Cymbopogon citratus* was dried successfully in the newly developed forced convection solar dryer. Based on the experimentally measured values, energy and exergy analyses of the drying process were performed. It was found that the *Cymbopogon citratus* sample was dried up to a final moisture content of approximately 0.09 kg water/kg dry matter with 0.055 kg/s mass flow rate of drying rate within 28 h and solar radiation intensity of 267.76 to 923.08 W/m^2. The energy taken from the solar collector was productively utilized inside the drying chamber. The drying chamber's higher exergy and lower thermal efficiency manifested considerable energy loss with the exhaust of the drying chamber. The lower mass flow of air was supplied to utilize the storage system's maximum capacity and obtain a constant heat supply for more prolonged nocturnal usage. The most efficient use of exergy was achieved when the losses were minimal. Compared to other drying techniques like direct type and open sun drying, the drying time is shorter with ISD. The air that exits the drying chamber has a high temperature that may be used by a secondary auxiliary drier or by any heat recovery system, providing many of future opportunities to increase the drying efficiency of the sample in developed ISD. The ISD may be constructed using locally accessible materials with minimal initial investment and in big enough quantities to increase the local community business's profit for the high-demand dried items like medicinal crops.

Acknowledgements The authors greatly acknowledge the research facility provided by the Department of Food Processing Technology at the Ghani Khan Choudhury Institute of Engineering and Technology, Malda, and Department of Food Engineering and Technology, Tezpur University, for giving the assistance required to carry out this research.

Author contribution Mohammed Abdullah Bareen: Writing original draft, reviewed, edited.
Soumya Dash: Writing original draft, reviewed, edited.
Paragmoni Kalita: Reviewed, edited.
Kshirod Kumar Dash: Conceptualized, writing original draft, reviewed, edited, supervision.

Data availability The datasets generated and analyzed during this study are available from the corresponding author on reasonable request.

Declarations

Ethics approval Not applicable.

Consent to participate Informed consent was obtained from all individual participants included in the study.

Consent to publish Not applicable.

Competing interests The authors declare no competing interests.

References

Abd Rahman N, Tasirin SM, Razak AHA, Mokhtar M, Muslim S (2013) Comparison of drying parameter optimization of lemon grass. World Appl Sci J 24(9):1234–1249. https://doi.org/10.5829/idosi.wasj.2013.24.09.1332

Agarwal A, Sarviya RM (2016) An experimental investigation of shell and tube latent heat storage for solar dryer using paraffin wax as heat storage material. Eng Sci Technol Int J 19(1):619–631. https://doi.org/10.1016/j.jestch.2015.09.014

Akbulut A, Durmuş A (2010) Energy and exergy analyses of thin layer drying of mulberry in a forced solar dryer. Energy 35(4):1754–1763. https://doi.org/10.1016/j.energy.2009.12.028

Alam PN, Husin H, Asnawi TM, Adisalamun (2018) Extraction of citral oil from lemongrass (Cymbopogon citratus) by steam-water distillation technique. IOP Conf Ser: Mater Sci Eng 345(1). https://doi.org/10.1088/1757-899X/345/1/012022

Alis RR, Rebustos MR, Abisate KA, Constantino J (2019) Solar-dried locally-available raw materials for food processing. Philipp J Crop Sci (Philippines) 44(1):163–174

Balti MA, Hadrich B, Kriaa K (2018) Lab-scale extraction of essential oils from Tunisian lemongrass (Cymbopogon flexuosus). Chem

Eng Process: Process Intensification 124(November 2017):164–173. https://doi.org/10.1016/j.cep.2017.12.012
Bhardwaj AK, Chauhan R, Kumar R, Sethi M, Rana A (2017) Experimental investigation of an indirect solar dryer integrated with phase change material for drying valeriana jatamansi (medicinal herb). Case Stud Therm Eng 10(March):302–314. https://doi.org/10.1016/j.csite.2017.07.009
Bhardwaj AK, Kumar R, Kumar S, Goel B, Chauhan R (2021) Energy and exergy analyses of drying medicinal herb in a novel forced convection solar dryer integrated with SHSM and PCM. Sustain Energy Technol Assess 45(February):101119. https://doi.org/10.1016/j.seta.2021.101119
Bouadila S, Kooli S, Skouri S, Lazaar M, Farhat A (2014) Improvement of the greenhouse climate using a solar air heater with latent storage energy. Energy 64:663–672. https://doi.org/10.1016/j.energy.2013.10.066
Boukhatem MN, Ferhat MA, Rajabi M, Mousa SA (2022) Solvent-free microwave extraction: an eco-friendly and rapid process for green isolation of essential oil from lemongrass. Nat Prod Res 36(2):664–667. https://doi.org/10.1080/14786419.2020.1795852
Celma AR, Cuadros F (2009) Energy and exergy analyses of OMW solar drying process. Renew Energy 34(3):660–666. https://doi.org/10.1016/j.renene.2008.05.019
Chauhan R, Kumar R, Bhardwaj AK, Rana A, Sethi M (2017) Experimental investigation of an indirect solar dryer integrated with phase change material for drying valeriana jatamansi (medicinal herb). Case Stud Therm Eng 10(March):302–314. https://doi.org/10.1016/j.csite.2017.07.009
Cheenkachorn K, Paulraj MG, Tantayotai P, Phakeenuya V, Sriariyanun M (2022) Characterization of biologically active compounds from different herbs: influence of drying and extraction methods. J Indian Chem Soc 99(1):100297. https://doi.org/10.1016/j.jics.2021.100297
Daniel M (2006) Medicinal plants: chemistry and properties, 1st edn. Science publishers. CRC Press, Boca Raton, pp 71–89
Darvishi H, Zarein M, Minaei S, Khafajeh H (2014) Exergy and energy analysis, drying kinetics and mathematical modeling of white mulberry drying process. Int J Food Eng 10(2):269–280
Dash S, Choudhury S, Dash KK (2022) Energy and exergy analyses of solar drying of black cardamom (Amomum subulatom Roxburgh) using indirect type flat plate collector solar dryer. J Food Process Eng 45(4):1–12. https://doi.org/10.1111/jfpe.14001
Dincer I, Rosen MA, Exergy E (2007) Environment and sustainable development. Elsevier
Ebaid MT (2011) Different methods to extract volatile oil from leaves of different medical plants. J Soil Sci Agric Eng 2(11):1141–1153. https://doi.org/10.21608/jssae.2011.56444
Ekechukwu OV, Norton B (1999) Review of solar-energy drying systems II: an overview of solar drying technology. Energy Convers Manag 40(6):615–655
El Khadraoui A, Bouadila S, Kooli S, Farhat A, Guizani A (2017) Thermal behavior of indirect solar dryer: nocturnal usage of solar air collector with PCM. J Clean Prod 148:37–48. https://doi.org/10.1016/j.jclepro.2017.01.149
El-Sebaii AA, Aboul-Enein S, Ramadan MRI, Shalaby SM, Moharram BM (2011) Thermal performance investigation of double pass-finned plate solar air heater. Appl Energy 88(5):1727–1739
Esakkimuthu S, Hassabou AH, Palaniappan C, Spinnler M, Blumenberg J, Velraj R (2013) Experimental investigation on phase change material based thermal storage system for solar air heating applications. Sol Energy 88:144–153
Fadhel MI, Sopian K, Daud WRW (2010) Performance analysis of solar-assisted chemical heat-pump dryer. Sol Energy 84(11):1920–1928. https://doi.org/10.1016/j.solener.2010.07.001
Fudholi A, Sopian K, Othman MY, Ruslan MH (2014) Energy and exergy analyses of solar drying system of red seaweed. Energy Build 68(PARTA):121–129. https://doi.org/10.1016/j.enbuild.2013.07.072
Ibrahim M, Sopian K, Daud WRW (2009) Study of the drying kinetics of lemon grass. Am J Appl Sci 6(6):1070
Jain D, Tewari P (2015) Performance of indirect through pass natural convective solar crop dryer with phase change thermal energy storage. Renew Energy 80:244–250
Janjai S, Chantaraksa W, Hirunlabh J, Esper A, Lauer M, Muehlbauer W (2002) Investigation of the performance of a solar dryer for lemon-grass. Proc Int Symp"Sustaining Food Secur Manag Nat Resour Southeast Asia Challenges 21st Century, pp 81–83
Karakaplan N, Goz E, Tosun E, Yuceer M (2019) Kinetic and artificial neural network modeling techniques to predict the drying kinetics of Mentha spicata L. J Food Process Preserv 43(10):1–10. https://doi.org/10.1111/jfpp.14142
Kaur G, Kaur P, Kaur A (2021) Preserving bioactive quality and color of novel frozen lemongrass puree tablets. In J Food Process Preserv. https://doi.org/10.1111/jfpp.16050
Khaerunnisa MM, Asfar M (2021) Characteristics of simplicia ginger (Zingiber officinale) and lemongrass (Cymbopogon citratus) powder by different drying method. IOP Conf Ser: Earth Environ Sci 807(2). https://doi.org/10.1088/1755-1315/807/2/022052
Kline SJ (1953) Describing uncertainty in single sample experiments. Mech Eng 75:3–8
Mabai P, Omolola A, Jideani AIO (2018) Effect of drying on quality and sensory attributes of lemongrass (Cymbopogon citratus) tea. J Food Res 7(2):68. https://doi.org/10.5539/jfr.v7n2p68
MacPhee D, Dincer I (2009) Thermal modeling of a packed bed thermal energy storage system during charging. Appl Therm Eng 29(4):695–705
Martins WS da, de Araújo JSF, Feitosa BF, Oliveira JR, Kotzebue LRV, Agostini DLS da, de Oliveira DLV, Mazzetto SE, Cavalcanti MT, da Silva AL (2021) Lemongrass (Cymbopogon citratus DC. Stapf) essential oil microparticles: development, characterization, and antioxidant potential. Food Chem 355(December 2020). https://doi.org/10.1016/j.foodchem.2021.129644
Mehta P, Samaddar S, Patel P, Markam B, Maiti S (2018) Design and performance analysis of a mixed mode tent-type solar dryer for fish-drying in coastal areas. Sol Energy 170:671–681
Mehta P, Bhatt N, Bassan G, Kabeel AE (2022a) Performance improvement and advancement studies of mixed-mode solar thermal dryers: a review. Environ Sci Pollut Res 1–17
Mehta P, Bhatt N, Bassan G, Kabeel AE (2022) Performance improvement and advancement studies of mixed-mode solar thermal dryers: a review. Environ Sci Pollut Res 29(42):62822–62838. https://doi.org/10.1007/s11356-022-21736-3
Mujaffar S, John S (2018) Thin-layer drying behavior of West Indian lemongrass (Cymbopogan citratus) leaves. Food Sci Nutr 6(4):1085–1099. https://doi.org/10.1002/fsn3.642
Nguyen TVL, Nguyen MD, Nguyen DC, Bach LG, Lam TD (2019) Model for thin layer drying of lemongrass (Cymbopogon citratus) by hot air. Processes7(1). https://doi.org/10.3390/pr7010021
Nur Ain AH, Zaibunnisa AH, Halimahton Zahrah MS, Norashikin S (2013) An experimental design approach for the extraction of lemongrass (Cymbopogon citratus) oleoresin using pressurised liquid extraction (PLE). Int Food Res J 20(1):451–455
Öztürk HH (2004) Experimental determination of energy and exergy efficiency of the solar parabolic-cooker. Sol Energy 77(1):67–71
Rabha DK, Muthukumar P, Somayaji C (2017) Energy and exergy analyses of the solar drying processes of ghost chilli pepper and ginger. Renew Energy 105:764–773
Ranganna S (1986) Handbook of analysis and quality control for fruit and vegetable products, 2nd edn. Tata McGraw-Hill Education, New York

Reyes A, Mahn A, Vásquez F (2014) Mushrooms dehydration in a hybrid-solar dryer, using a phase change material. Energy Convers Manag 83:241–248. https://doi.org/10.1016/j.enconman.2014.03.077

Shalaby SM, Bek MA (2014) Experimental investigation of a novel indirect solar dryer implementing PCM as energy storage medium. Energy Convers Manag 83:1–8. https://doi.org/10.1016/j.enconman.2014.03.043

Singh S, Kumar S (2012) Testing method for thermal performance based rating of various solar dryer designs. Sol Energy 86(1):87–98. https://doi.org/10.1016/j.solener.2011.09.009

Thuong Nhan NP, Thanh VT, Cang MH, Lam TD, Huong NC, Hong Nhan LT, Truc TT, Tran QT, Bach LG (2020) Microencapsulation of lemongrass (Cymbopogon citratus) essential oil via spray drying: effects of feed emulsion parameters. Processes 8(1). https://doi.org/10.3390/pr8010040

Tiwari GN, Suneja S (1997) Solar thermal engineering systems. Narosa Publishing House, New Delhi, pp 81–83

Torres-reyes E, Gortari JGC, Ibarra-salazar BA, Picon-nuñez M (2001) A design method of flat-plate solar collectors based on. Entropy 1(1):46–52